Obstacle-avoidance verification for a switched control strategy

Ray Essick

***Abstract*—We present a case study of a trajectory regulation problem for a three degrees-of-freedom helicopter system which approaches an obstacle during operation. While the helicopter is close to the obstacle, the controller strategy must focus on a "critical output" to prevent a collision. We first model the nonlinear helicopter plant as a switched linear system whose modes correspond to operation near to and far from the obstacle. A recent result in controller synthesis for switched systems is used to determine a suitable controller for guaranteeing closed-loop stability and a performance gain. The closed-loop system is then modeled as a hybrid system which is analyzed using SpaceEx. An overapproximation of the reachable set is computed, but is insufficient to guarantee the collision-avoidance property, suggesting modifications to the hybrid model used.**

I. Introduction

The hybrid systems model is increasingly used as a means of combining continuous-state dynamics with discrete logic to model complex systems such as networked control systems ([5], [8]), distributed networks of autonomous vehicles ([7], [9]), and biological and chemical processes ([1], [11]). Methods of designing controllers for such systems focus principally on stabilization and also minimizing some output criterion, often either the system norm (ℓ_2-induced) or output variance. While a number of techniques exist for guaranteeing these properties, they are typically focused on the steady-state or long-term behavior of the system, with few guarantees on transient system performance. The verification of hybrid systems, on the other hand, often focuses on the proving of invariant sets within which the reachable states of the system are contained. Such results give a proof that system safety properties, such as collision avoidance, are correct with little information on the evolution of the system within the reachable states.

We wish to combine the tools from both control theory and hybrid systems verification to design a controller which achieves good trajectory tracking while also guaranteeing collision avoidance. We will consider the three degrees-of-freedom helicopter plant shown in Figure 1 for our study. During operation, the helicopter will pass close to an obstacle, presenting the possibility of a collision. We will develop a linear model for the system with switching dynamics, and use a recent result in switched system theory to synthesize a suitable controller which guarantees trajectory tracking. We will then implement the closed-loop system in the SpaceEx analysis tool and attempt to verify the reachable set of the system. Although our analysis does not guarantee the collision-avoidance property we are seeking, we will present several options for future development in this area.

R. Essick is with the Department of Mechanical Science and Engineering, University of Illinois at Urbana-Champaign, Urbana, IL 61801 USA

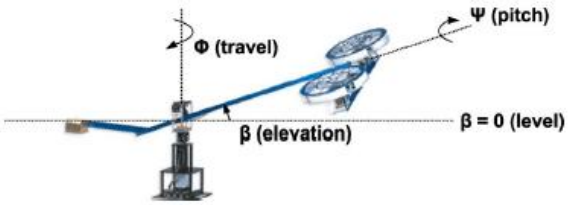

Fig. 1. The Quansar 3DOF helicopter plant

We begin by reviewing our result for controller synthesis for switched linear systems in Section II. Next, in Section III we will develop the dynamics of the 3DOF helicopter system and design our controller. In Section IV we will outline the modeling scheme used in SpaceEx. Finally, Section V presents an outline of future work for effective reachability verification.

II. Disturbance attenuation in switched systems

A switched linear system is an LTV system whose parameters at each time step are selected from a finite set. That is, the system parameters are described by an indexed set

$$\{(A_i, B_{1,i}, B_{2,i}, C_{1,i}, C_{2,i}, D_{11,i}, D_{12,i}, D_{21,i})\}, \quad i = 1, \ldots, N \tag{1}$$

and governed by dynamics of the form

$$\begin{aligned} x_{t+1} &= A_{\theta(t)}x_t + B_{1,\theta(t)}w_t + B_{2,\theta(t)}u_t \\ z_t &= C_{1,\theta(t)}x_t + D_{11,\theta(t)}w_t + D_{12,\theta(t)}u_t \\ y_t &= C_{2,\theta(t)}x_t + D_{21,\theta(t)}w_t \end{aligned} \tag{2}$$

Here the sequence $\theta : \mathbb{Z}^+ \to \{1, \ldots, N\}$ is a switching sequence that determines, at each time $t \geq 0$, which of the system parameters are used at that time. The switching dynamics are described by a matrix $Q \in \{0,1\}^{N \times N}$, which represents the adjacency matrix of a directed graph. An *admissible switching sequence* is a sequence (finite or infinite) which represents a valid walk through this directed graph. Throughout this paper we will assume that Q is a strongly connected graph; that is, a path exists between any two modes.

Definition 1: A switched linear system is called uniformly exponentially stable there exist constants $c \geq 1$ and $\lambda \in (0,1)$ such that for every admissible switching sequence θ and all $k \geq 0$

$$\|A_{\theta(t+k)} \cdot \ldots \cdot A_{\theta(t)}\| \leq c\lambda^k \tag{3}$$

for all $t \geq 0$.

In addition to examining the stability of the system, we also wish to bound the ℓ_2-induced system norm from disturbance input w to controlled output z for the system, according to the following definition.

Definition 2: A switched linear system satisfies disturbance attenuation level $\gamma > 0$ if for every admissible switching sequence θ, the system satisfies

$$\|z\|_2^2 < \gamma^2 \|w\|_2^2 \tag{4}$$

or, equivalently, if the system satisfies

$$\sup_w \frac{\|z\|}{\|w\|} < \gamma$$

We will connect this system in output feedback with a *finite-path dependent* controller. The controller is given access to the observed output y_t at each time, as well as access to a portion of the switching signal. We permit perfect observation and memory of the current mode and $L \geq 0$ past modes; we also allow a preview of $H \geq 0$ future switching modes. The resulting controller gains are dependent on the finite-length switching signal $\theta_{(t-L:t+H)} = (\theta(t-L), \ldots, \theta(t+H))$ and yield the following controller dynamics.

$$\begin{aligned} \hat{x}_{t+1} &= \hat{A}_{\theta_{(t-L:t+H)}} \hat{x}_t + \hat{B}_{\theta_{(t-L:t+H)}} y_t \\ u_t &= \hat{C}_{\theta_{(t-L:t+H)}} \hat{x}_t + \hat{D}_{\theta_{(t-L:t+H)}} y_t \end{aligned} \tag{5}$$

The existence of such a controller such that the closed-loop system is both uniformly exponentially stable and uniformly strictly contractive is characterized in the following result (from [4]) in the form of a family of semidefinite programming problems.

Theorem 3: There exists a controller with memory $L \geq 0$ and horizon $H \geq 0$ achieving uniform stabilization and attenuation level γ for the closed-loop system of (**??**) if and only if there exist an integer $M \geq 0$ and matrices $R_j \succ 0$, $S_j \succ 0$ for $j \in \{1, \ldots, N\}^{L+M+H}$ such that

$$\begin{aligned} &\begin{bmatrix} N_{F,i_0} & 0 \\ 0 & I \end{bmatrix}^T \\ &\times \begin{bmatrix} A_{i_0} R_{i_{(-L-M:H-1)}} A_{i_0}^T - R_{i_{(-L-M+1:H)}} \\ C_{1,i_0} R_{i_{(-L-M:H-1)}} A_{i_0}^T \\ B_{1,i_0}^T \end{bmatrix} \\ &\qquad \begin{bmatrix} A_{i_0} R_{i_{(-L-M:H-1)}} C_{1,i_0}^T & B_{1,i_0} \\ C_{1,i_0} R_{i_{(-L-M:H-1)}} C_{1,i_0}^T - \gamma I & D_{11,i_0} \\ D_{11,i_0}^T & -\gamma I \end{bmatrix} \\ &\times \begin{bmatrix} N_{F,i_0} & 0 \\ 0 & I \end{bmatrix} \prec 0 \end{aligned} \tag{6a}$$

$$\begin{aligned} &\begin{bmatrix} N_{G,i_0} & 0 \\ 0 & I \end{bmatrix}^T \\ &\times \begin{bmatrix} A_{i_0}^T S_{i_{(-L-M+1:H)}} A_{i_0} - S_{i_{(-L-M:H-1)}} \\ B_{1,i_0}^T S_{i_{(-L-M+1:H)}} A_{i_0} \\ C_{1,i_0} \end{bmatrix} \\ &\qquad \begin{bmatrix} A_{i_0}^T S_{i_{(-L-M+1:H)}} B_{1,i_0} & C_{1,i_0}^T \\ B_{1,i_0}^T S_{i_{(-L-M+1:H)}} B_{1,i_0} - \gamma I & D_{11,i_0}^T \\ D_{11,i_0} & -\gamma I \end{bmatrix} \\ &\times \begin{bmatrix} N_{G,i_0} & 0 \\ 0 & I \end{bmatrix} \prec 0 \end{aligned} \tag{6b}$$

$$\begin{bmatrix} R_{i_{(-L-M:H-1)}} & I \\ I & S_{i_{(-L-M:H-1)}} \end{bmatrix} \succeq 0 \tag{6c}$$

for all admissible sequences $i_{(-L-M:H)}$, where the operator $N(X)$ denotes any full-rank matrix Y such that $\mathrm{Im}\,(X) = \mathrm{null}(y)$ and

$$N_{F,i} = N(\begin{bmatrix} B_{2,i}^T & D_{12,i}^T \end{bmatrix});\ N_{G,i} = N(\begin{bmatrix} C_{2,i} & D_{21,i} \end{bmatrix})$$

A feasible solution to the inequalities described above allows for the construction of a controller which guarantees both stability and disturbance attenuation. The controller existence and synthesis computations can all be completed offline, leading to a collection of controllers indexed by finite-length switching paths. Online implementation of the controller consists of observing the switching path information given at each time step and selecting the corresponding controller.

III. System modeling and controller synthesis

The system we wish to control is the 3DOF helicopter shown in Figure 1, which is a tabletop mounted system from Quanser Consulting [10]. The plant consists of a centrally mounted arm which may rotate freely about the base, with a counterweight at one end and the helicopter body at the other. The helicopter has two propellers which are joined by a nacelle which can rotate freely about the end of the arm. The travel ϕ denotes the rotation of the arm around the vertical axis through the base, measured positive in the clockwise direction when viewed from above. The elevation β gives the angular elevation of the bar, measured upwards from level. The pitch angle ψ denotes the rotation of the nacelle about the end of the arm, measured positive in the clockwise direction when viewed radially inward. We set $\beta = 0$ when the arm is level, $\psi = 0$ when the nacelle is level, and take $\phi = 0$ to be the arm travel at startup.

We begin by modeling the flight dynamics of the system. A nonlinear model of this system is developed in [3] and gives the following equations:

$$\ddot{\phi} = -0.0252\dot{\phi} - 0.0525 V_c^2 \sin(\psi - 0.0827) \tag{7}$$

$$\begin{aligned} \ddot{\beta} = &-0.112\dot{\beta} - 0.243\cos\beta - 0.504\sin\beta + 0.04\dot{\phi}^2 \\ &+ 0.0905 V_c^2 \cos\psi \end{aligned} \tag{8}$$

$$\ddot{\psi} = -0.163\dot{\psi} - 1.58\sin\psi + 0.131 - 0.449\dot{\psi}^2 + 1.42 V_c V_y \tag{9}$$

in which $V_c = V_f + V_r$ and $V_y = V_f - V_y$, where V_f and V_y denote the voltages to the front motor and rear motor. The voltages are measured in volts, all angles are measured in radians, and time is measured in seconds. We wish to control the helicopter along the reference trajectory of $\dot{\phi}_r = -1$ rad/s and $\beta_r = 0.2618$ rad. As the helicopter moves along this trajectory, an obstacle is introduced in the form of a box whose height is slightly less than that of the reference trajectory. When the helicopter is operating near the box, the elevation of the helicopter (specifically, of the leading edge of the nacelle) is a critical output of the system for avoiding a collision.

We now develop a linearized model of the system above, which is based on the linear hover model found in [3]. For this hover model all angular velocities are set to zero, while the elevation angle $\beta = \beta_r$ is set to our reference elevation. The pitch angle ψ must be set to 0.0827 radians to counterbalance the net torque caused by the two propellers. To these dynamics we add a disturbance input w, which can affect each of the three degrees of freedom independently. The resulting linear system has inputs $\bar{V_c}$ and $\bar{V_y}$, and introduces two torques $\bar{\tau_c}$ and $\bar{\tau_y}$, with the resulting linearized dynamics:

$$\begin{aligned}
\dot{\bar{\tau_c}} &= -6.16\bar{\tau_c} + \bar{V_c} \\
\dot{\bar{\tau_y}} &= -7.32\bar{\tau_y} + \bar{V_y} \\
\ddot{\bar{\phi}} &= -0.0839\dot{\bar{\phi}} - 0.257\bar{\psi} + w_1 \\
\ddot{\bar{\beta}} &= -0.112\dot{\bar{\beta}} - 0.504\bar{\beta} + 1.34\bar{\tau_c} + w_2 \\
\ddot{\bar{\psi}} &= -0.163\dot{\bar{\psi}} - 1.58\bar{\psi} + 16.2\bar{\tau_y} + w_3
\end{aligned}$$

We will introduce one additional state which is related to the position of the front corner of the helicopter nacelle. While the helicopter is following the reference trajectory, this corner is the lowest point on the body of the helicopter and therefore critical for collision avoidance. The vertical position of this corner above the plane where $\beta = 0$ is given by $\zeta = 0.66 \sin\beta - 0.277 \sin\psi$. We will define the integral state $\bar{\xi}$ with the dynamics $\dot{\bar{x}}i = (0.66)\cos\beta_r\bar{\beta} - 0.277\cos\psi_r\bar{\psi} = \bar{\zeta}$.

The resulting system has the state vector $x = \left[\bar{\phi}, \bar{\beta}, \bar{\psi}, \dot{\bar{\phi}}, \dot{\bar{\beta}}, \dot{\bar{\psi}}, \tau_c, \tau_y, \xi\right]$, along with the disturbance w and input $u = \begin{bmatrix} V_c & V_y \end{bmatrix}$ and obeys the continuous-time dynamics described above. We discretize these dynamics with a time interval $h = 0.05s$ to produce a discrete-time system.

During operation, the helicopter trajectory will pass directly above a box whose height is only slightly below the reference height for the system. While the helicopter is flying above the box, guaranteeing collision avoidance becomes the most important property for the system. The front corner of the helicopter nacelle, described by ζ above, represents the lowest point on the model and therefore the point where a collision will occur. It is therefore important that the controller focus on this "critical" output while near an obstacle.

From the dynamics of the system, it is clear that a trade-off must be made between tracking the reference angular velocity $\dot{\phi}_r$ and the reference height β_r; increasing the height of the helicopter beta involves reducing the nacelle angle ψ and slowing the system down, while increasing the speed $\dot{\phi}$ requires increasing this angle and lowering the altitude. In order that the controller favor altitude control while near an obstacle, we introduce a controlled output which weights these two criteria according to some danger parameter δ. We suppose that δ is some function of distance to the obstacle, with $\delta = 0$ when far from the box and $\delta = 1$ while directly over it. We then introduce the controlled output of the system given by

$$z = \begin{bmatrix} (1 - 0.9\delta)(\dot{\bar{\phi}} + 0.5\bar{\phi}) \\ (1 + 0.9\delta)(\zeta + 0.1\xi) \\ 0.25V_c \\ 0.25V_y \end{bmatrix} \tag{10}$$

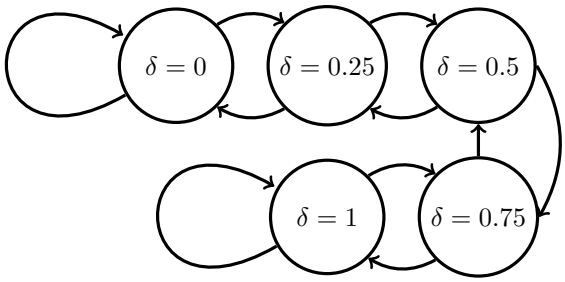

Fig. 2. The switching graph between modes for the controlled output of the system.

Using this output, when the helicopter is far from the obstacle ($\delta = 0$) the two reference objectives of altitude (ζ, ξ) and velocity $(\bar{\phi}, \dot{\bar{\phi}})$ are penalized equally. When near the obstacle ($\delta = 1$) the altitude of the helicopter is weighted much more significantly than the velocity.

While the parameter δ could be taken as a continuous function of helicopter position, we introduce discrete levels to produce a finite number of system modes and corresponding outputs. There is a design trade-off made here between the complexity of the model and the precise location of the helicopter relative to the obstacle. In order to balance these two considerations, we give our system a total of five modes, corresponding to δ values of $0, 0.25, 0.5, 0.75$, and 1. In each mode the system dynamics remain the same, as does the observed output $y = \left[\phi, \beta, \psi, \xi\right]$. Since we assume that the helicopter approaches and leaves the obstacle in a smooth way, we will suppose that the system may transition from adjacent values of δ, or else remain at a value of $\delta = 0$ or 1. The resulting switching graph is shown in Figure 2.

We have now modeled our system as a switched linear system, and can apply the result of Theorem 3 to search for a suitable controller. We discover that the simplest possible case, a modal controller, exists which achieves a system norm of $\gamma = 2.5$. Searching for a path-dependent controller produces more complex controllers which can reduce this value slightly; however, this improved performance comes at an increase in the number of controller modes and memory. Since very little time will be spent where the controller is switching between $\delta = 0$ and $\delta = 1$, the added complexity will not help with performance near the obstacle. We therefore settle for the modal controller, which has five modes and nine states of its own. The gains selected are given in the appendix.

IV. Closed-loop safety verification

With a controller in hand, we move to the collision-avoidance verification problem. Our approach is to model the closed-loop system as a hybrid system using the SpaceEx analysis tool and attempt to compute the reachable set of system states. Ideally, no element of this set will have a value of ζ large enough to cause a collision.

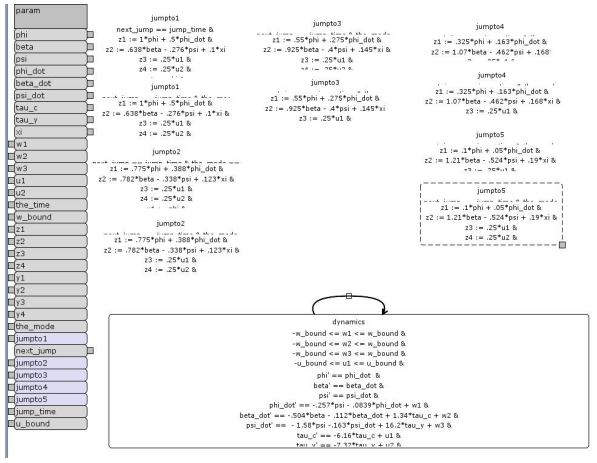

Fig. 3. The SpaceEx helicopter model.

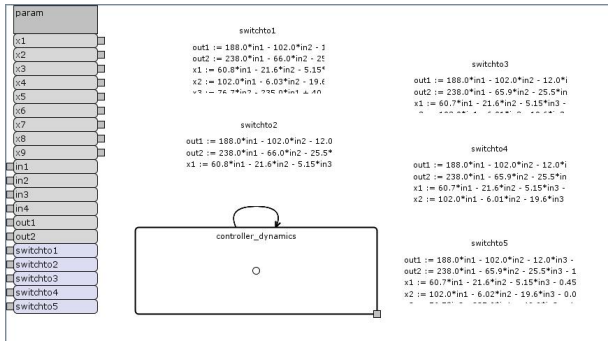

Fig. 4. The SpaceEx controller model.

The SpaceEx modeling framework allows us to construct separate hybrid systems for the helicopter plant and controller, and then network them together to form a composite hybrid system. We take this approach to allow for easy modification of either the plant dynamics or control law independent of the other component. Since the plant dynamics are identical for every output mode, we model the helicopter with a single mode under which the system states evolve according to the continuous-time dynamics of Section III. This single mode is paired with transitions corresponding to switching *into* each of the five output modes. At each time step, the system follows one of these transitions and updates the values of both the controlled and observed outputs, as well as a variable storing the current mode. The values of the outputs remain constant between information updates, as the controller dynamics are still discrete. Figure 3 shows a graphical representation of the helicopter model.

The controller dynamics remain discrete and the control output from the controller remains constant between updates, so the controller is also modeled as a single mode with transitions for updating the controller state and control output. When the plant takes a transition, the controller takes the corresponding transition and updates the control law and its internal state according to the newly updated observed output of the system. The SpaceEx model for the controller is shown in Figure 4

The helicopter and controller model are connected together to form a feedback loop, providing a composite hybrid system which accepts as inputs the disturbances w_1, w_2, w_3 and as outputs the controlled components z_1, z_2, z_3, z_4. Uniform bounds are placed on the magnitude of the disturbances at each time step, and the resulting system is simulated to determine an approximation of the feasible set. The analysis was run on a laptop featuring a 1.5 Ghz processor with 4 Gb of memory, implementing a virtual Linux machine with access to 1 Gb of memory.

The resulting feasibility analysis of this hybrid model proved almost completely unusable for determining a bound on the magnitude of the nacelle position ζ. Repeated analysis of the model yielded either an overly conservative approximation which could not tightly bound the behavior of the system, or else quickly became intractable.

V. Future Work

Despite the failure of our initial model to tightly bound the reachable set of states, several promising alterations are suggested by the errors we faced. First, in order to ensure good performance for stabilization, the switching controller was designed with a time step of $h = 0.05s$, allowing the controller to rapidly switch. In modeling the dynamics of the helicopter, we produce an observed output each time step, but additionally allow the system mode to switch at this frequency. As a result, the model we simulate may switch between being far from ($\delta = 0$) and near to ($\delta = 1$) the obstacle as often as every 0.25 seconds. This switching rate is much faster than we would normally see as the physical system approaches a real obstacle. Modifying the system such that the controller updates very quickly, while the plant mode switches on a much slower time scale would greatly reduce the growth of reachable states due to switching. Alternately, we could use multiple timers to enforce a particular output switching to correspond to some fixed obstacle approach. This approach would effectively eliminate the nondeterminism from the system switching, however, and require that the simulation be run for many different possible obstacle profiles in order to verify obstacle avoidance.

In addition, the model fails to correctly limit the disturbance signal w to correspond to a bounded (in the 2-norm) signal. The controller design cannot uniformly bound system output for any disturbance; the bound is a function of the norm of the disturbance. In order to accurately predict the collision properties of the system, we should place bounds on the norm of w rather than on the magnitude at each time step. Finding a way to properly measure and bound the 2-norm of a signal in SpaceEx will improve future models.

Appendix

The controller design uses five modes, according to the feedback law

$$\hat{x}_{t+1} = \hat{A}_{\theta(t)}\hat{x}_t + \hat{B}_{\theta(t)}y_t$$
$$u_t = \hat{C}_{\theta(t)}\hat{x}_t + \hat{D}_{\theta(t)}y_t$$

The gains for each controller mode are given by:

$$A_1 = \begin{bmatrix} 0.279 & -0.016 & -0.020 & -0.012 & -0.020 \\ -1.063 & 0.388 & -0.104 & 0.009 & -0.099 \\ 2.689 & 0.309 & 0.779 & 0.037 & 0.202 \\ 3.368 & -0.737 & -0.156 & 0.788 & 0.048 \\ 2.773 & 0.347 & 0.174 & 0.035 & 0.649 \\ -0.004 & 0.002 & 0.001 & -0.000 & -0.000 \\ 0.511 & -0.017 & 0.424 & 0.005 & -0.169 \\ -0.091 & 0.374 & 0.084 & -0.022 & 0.042 \\ 0.002 & -0.000 & 0.000 & 0.000 & 0.000 \end{bmatrix}$$

$$\begin{bmatrix} 0.000 & -0.002 & -0.011 & 0.000 \\ 0.001 & -0.058 & 0.126 & -0.002 \\ 0.001 & 0.274 & 0.314 & 0.006 \\ -0.003 & -0.043 & -0.458 & 0.007 \\ 0.000 & -0.170 & 0.300 & 0.006 \\ 0.005 & -0.000 & -0.001 & -0.000 \\ 0.001 & 0.316 & 0.039 & 0.001 \\ 0.001 & -0.009 & 0.232 & -0.000 \\ -0.000 & 0.000 & 0.000 & 0.000 \end{bmatrix}$$

$$A_2 = \begin{bmatrix} 0.279 & -0.016 & -0.020 & -0.012 & -0.020 \\ -1.062 & 0.388 & -0.104 & 0.009 & -0.099 \\ 2.687 & 0.308 & 0.779 & 0.037 & 0.202 \\ 3.366 & -0.737 & -0.157 & 0.788 & 0.048 \\ 2.771 & 0.346 & 0.174 & 0.035 & 0.649 \\ -0.004 & 0.002 & 0.001 & -0.000 & -0.000 \\ 0.511 & -0.017 & 0.424 & 0.005 & -0.169 \\ -0.091 & 0.374 & 0.084 & -0.022 & 0.042 \\ 0.002 & -0.000 & 0.000 & 0.000 & 0.000 \end{bmatrix}$$

$$\begin{bmatrix} 0.000 & -0.002 & -0.011 & 0.000 \\ 0.001 & -0.058 & 0.126 & -0.002 \\ 0.001 & 0.274 & 0.314 & 0.006 \\ -0.003 & -0.044 & -0.459 & 0.007 \\ 0.000 & -0.170 & 0.299 & 0.006 \\ 0.005 & -0.000 & -0.001 & -0.000 \\ 0.001 & 0.316 & 0.039 & 0.001 \\ 0.001 & -0.009 & 0.232 & -0.000 \\ -0.000 & 0.000 & 0.000 & 0.000 \end{bmatrix}$$

$$A_3 = \begin{bmatrix} 0.279 & -0.016 & -0.020 & -0.012 & -0.020 \\ -1.062 & 0.388 & -0.104 & 0.009 & -0.099 \\ 2.685 & 0.308 & 0.779 & 0.037 & 0.202 \\ 3.365 & -0.738 & -0.157 & 0.788 & 0.048 \\ 2.770 & 0.346 & 0.174 & 0.035 & 0.649 \\ -0.004 & 0.002 & 0.001 & -0.000 & -0.000 \\ 0.511 & -0.017 & 0.424 & 0.005 & -0.169 \\ -0.092 & 0.374 & 0.084 & -0.022 & 0.042 \\ 0.002 & -0.000 & 0.000 & 0.000 & 0.000 \end{bmatrix}$$

$$\begin{bmatrix} 0.000 & -0.002 & -0.011 & 0.000 \\ 0.001 & -0.058 & 0.126 & -0.002 \\ 0.001 & 0.273 & 0.314 & 0.006 \\ -0.003 & -0.044 & -0.459 & 0.007 \\ 0.000 & -0.171 & 0.299 & 0.006 \\ 0.005 & -0.000 & -0.001 & -0.000 \\ 0.001 & 0.316 & 0.039 & 0.001 \\ 0.001 & -0.009 & 0.232 & -0.000 \\ -0.000 & 0.000 & 0.000 & 0.000 \end{bmatrix}$$

$$A_4 = \begin{bmatrix} 0.279 & -0.016 & -0.020 & -0.012 & -0.020 \\ -1.061 & 0.388 & -0.104 & 0.009 & -0.099 \\ 2.685 & 0.308 & 0.779 & 0.037 & 0.202 \\ 3.365 & -0.738 & -0.157 & 0.788 & 0.048 \\ 2.770 & 0.346 & 0.174 & 0.035 & 0.649 \\ -0.004 & 0.002 & 0.001 & -0.000 & -0.000 \\ 0.510 & -0.017 & 0.424 & 0.005 & -0.169 \\ -0.092 & 0.374 & 0.084 & -0.022 & 0.042 \\ 0.002 & -0.000 & 0.000 & 0.000 & 0.000 \end{bmatrix}$$

$$\begin{bmatrix} 0.000 & -0.002 & -0.011 & 0.000 \\ 0.001 & -0.058 & 0.126 & -0.002 \\ 0.001 & 0.273 & 0.314 & 0.006 \\ -0.003 & -0.044 & -0.459 & 0.007 \\ 0.000 & -0.171 & 0.299 & 0.006 \\ 0.005 & -0.000 & -0.001 & -0.000 \\ 0.001 & 0.316 & 0.039 & 0.001 \\ 0.001 & -0.009 & 0.232 & -0.000 \\ -0.000 & 0.000 & 0.000 & 0.000 \end{bmatrix}$$

$$A_5 = \begin{bmatrix} 0.279 & -0.016 & -0.020 & -0.012 & -0.020 \\ -1.062 & 0.388 & -0.104 & 0.009 & -0.099 \\ 2.685 & 0.308 & 0.778 & 0.037 & 0.202 \\ 3.365 & -0.738 & -0.157 & 0.788 & 0.048 \\ 2.769 & 0.346 & 0.174 & 0.035 & 0.649 \\ -0.004 & 0.002 & 0.001 & -0.000 & -0.000 \\ 0.510 & -0.017 & 0.424 & 0.005 & -0.169 \\ -0.092 & 0.374 & 0.084 & -0.022 & 0.042 \\ 0.002 & -0.000 & 0.000 & 0.000 & 0.000 \end{bmatrix}$$

$$\begin{bmatrix} 0.000 & -0.002 & -0.011 & 0.000 \\ 0.001 & -0.058 & 0.126 & -0.002 \\ 0.001 & 0.273 & 0.314 & 0.006 \\ -0.003 & -0.044 & -0.459 & 0.007 \\ 0.000 & -0.171 & 0.299 & 0.006 \\ 0.005 & -0.000 & -0.001 & -0.000 \\ 0.001 & 0.316 & 0.039 & 0.001 \\ 0.001 & -0.009 & 0.232 & -0.000 \\ -0.000 & 0.000 & 0.000 & 0.000 \end{bmatrix}$$

$$B_1 = \begin{bmatrix} 60.789 & -21.646 & -5.153 & -0.452 \\ 102.078 & -6.032 & -19.601 & -0.044 \\ -235.122 & 76.737 & 40.908 & 1.604 \\ -273.130 & 148.481 & 17.368 & 5.632 \\ -247.681 & 69.853 & 16.293 & 1.694 \\ 0.307 & 0.247 & -0.218 & 30.393 \\ -48.905 & 8.406 & -14.104 & 0.350 \\ 2.124 & -19.498 & 4.249 & -0.392 \\ -0.173 & 0.066 & 0.012 & 0.001 \end{bmatrix}$$

$$B_2 = \begin{bmatrix} 60.756 & -21.638 & -5.150 & -0.452 \\ 101.984 & -6.016 & -19.594 & -0.044 \\ -234.905 & 76.697 & 40.895 & 1.603 \\ -272.954 & 148.450 & 17.358 & 5.631 \\ -247.474 & 69.814 & 16.281 & 1.693 \\ 0.307 & 0.247 & -0.217 & 30.393 \\ -48.866 & 8.399 & -14.106 & 0.350 \\ 2.134 & -19.500 & 4.248 & -0.392 \\ -0.173 & 0.066 & 0.012 & 0.001 \end{bmatrix}$$

$$B_3 = \begin{bmatrix} 60.743 & -21.636 & -5.148 & -0.452 \\ 101.930 & -6.009 & -19.591 & -0.044 \\ -234.764 & 76.673 & 40.887 & 1.603 \\ -272.846 & 148.434 & 17.352 & 5.631 \\ -247.342 & 69.792 & 16.274 & 1.692 \\ 0.307 & 0.247 & -0.218 & 30.393 \\ -48.842 & 8.394 & -14.107 & 0.350 \\ 2.141 & -19.501 & 4.248 & -0.392 \\ -0.173 & 0.065 & 0.012 & 0.001 \end{bmatrix}$$

$$B_4 = \begin{bmatrix} 60.741 & -21.636 & -5.148 & -0.452 \\ 101.911 & -6.011 & -19.590 & -0.044 \\ -234.690 & 76.664 & 40.883 & 1.603 \\ -272.793 & 148.431 & 17.349 & 5.631 \\ -247.274 & 69.783 & 16.271 & 1.692 \\ 0.308 & 0.246 & -0.218 & 30.393 \\ -48.831 & 8.392 & -14.108 & 0.350 \\ 2.144 & -19.501 & 4.247 & -0.392 \\ -0.173 & 0.065 & 0.012 & 0.001 \end{bmatrix}$$

$$B_5 = \begin{bmatrix} 60.747 & -21.640 & -5.148 & -0.452 \\ 101.921 & -6.021 & -19.591 & -0.045 \\ -234.667 & 76.666 & 40.882 & 1.603 \\ -272.782 & 148.438 & 17.348 & 5.632 \\ -247.257 & 69.786 & 16.270 & 1.693 \\ 0.312 & 0.245 & -0.218 & 30.393 \\ -48.830 & 8.393 & -14.107 & 0.350 \\ 2.144 & -19.500 & 4.247 & -0.392 \\ -0.173 & 0.065 & 0.012 & 0.001 \end{bmatrix}$$

$$C_1 = \begin{bmatrix} -2.316 & 0.494 & 0.104 & -0.037 & -0.031 \\ -2.667 & -0.366 & -0.155 & -0.030 & -0.059 \\ 0.001 & 0.028 & 0.291 & -0.005 \\ -0.001 & -0.026 & -0.261 & -0.006 \end{bmatrix}$$

$$C_2 = \begin{bmatrix} -2.315 & 0.494 & 0.104 & -0.037 & -0.031 \\ -2.665 & -0.365 & -0.155 & -0.030 & -0.058 \\ 0.001 & 0.028 & 0.291 & -0.005 \\ -0.001 & -0.025 & -0.261 & -0.006 \end{bmatrix}$$

$$C_3 = \begin{bmatrix} -2.314 & 0.494 & 0.105 & -0.037 & -0.031 \\ -2.664 & -0.365 & -0.155 & -0.030 & -0.058 \\ 0.001 & 0.029 & 0.291 & -0.005 \\ -0.001 & -0.025 & -0.261 & -0.006 \end{bmatrix}$$

$$C_4 = \begin{bmatrix} -2.314 & 0.495 & 0.105 & -0.037 & -0.031 \\ -2.664 & -0.365 & -0.155 & -0.030 & -0.058 \\ 0.001 & 0.029 & 0.291 & -0.005 \\ -0.001 & -0.025 & -0.260 & -0.006 \end{bmatrix}$$

$$C = \begin{bmatrix} -2.314 & 0.495 & 0.105 & -0.037 & -0.031 \\ -2.663 & -0.365 & -0.155 & -0.030 & -0.058 \\ 0.001 & 0.029 & 0.291 & -0.005 \\ -0.001 & -0.025 & -0.260 & -0.006 \end{bmatrix}$$

$$D_1 = \begin{bmatrix} 188.114 & -101.841 & -11.985 & -3.821 \\ 238.387 & -65.998 & -25.538 & -1.457 \end{bmatrix}$$

$$D_2 = \begin{bmatrix} 187.989 & -101.820 & -11.978 & -3.821 \\ 238.175 & -65.959 & -25.525 & -1.456 \end{bmatrix}$$

$$D_3 = \begin{bmatrix} 187.912 & -101.808 & -11.974 & -3.821 \\ 238.041 & -65.937 & -25.518 & -1.456 \end{bmatrix}$$

$$D_4 = \begin{bmatrix} 187.875 & -101.806 & -11.972 & -3.821 \\ 237.973 & -65.929 & -25.514 & -1.456 \end{bmatrix}$$

$$D_5 = \begin{bmatrix} 187.867 & -101.810 & -11.971 & -3.821 \\ 237.958 & -65.933 & -25.514 & -1.457 \end{bmatrix}$$

REFERENCES

[1] C. Alur, R.and Belta, V. Kumar, M. Mintz, G. J. Pappas, H. Rubin, and J. Schug. Modeling and analyzing biomolecular networks. *Computing in Science and Engineering*, 4:20–31, 2002.

[2] A. M. Bayen, I. Mitchell, M. K. Oishi, and C. J. Tomlin. Reachability analysis and optimal control applied to aircraft autoland systems. *AIAA Journal on Guidance, Control and Dynamics*, 30(1):68–77, 2007.

[3] C. W. Dever. *Parameterized maneuvers for autonomous vehicles*. PhD thesis, Dept. Mech. Eng., Massachusetts Inst. Technol.

[4] R. Essick, J.-W. Lee, and G. E. Dullerud. An exact convex solution to receding horizon control. In *Proceedings of the 2012 American Control Conference*, jun. 2012.

[5] V. Gupta, B. Hassibi, and R. M. Murray. Optimal LQG control across packet-dropping links. *Systems & Control Letters*, 56:439–446, 2007.

[6] I. Hwang, H. Balakrishnan, and C. J. Tomlin. State estimation for hybrid systems: Applications to aircraft tracking.

[7] A. Jadbabaie, J. Lin, and A. S. Morse. Coordination of groups of mobile autonomous agents using nearest-neighbor rules. *IEEE Transactions on Automatic Control*, 48:988–1001, 2003.

[8] R. Krtolica, U. Özgüner, H. Chan, H. Göktas, J. Winkelman, and M. Liubakka. Stability of linear feedback systems with random communication delays. *International Journal of Control*, 59:925–953, 1994.

[9] R. Olfati-Saber, J. A. Fax, and R. M. Murray. Consensus and cooperation in networked multi-agent systems. *Proceedings of the IEEE*, 95:215–233, 2007.

[10] Quansar Consulting. *3D helicopter system (with active disturbance)*. Markham, ON, Canada, 2003. User's Manual.

[11] H. Salis and Y. Kaznessis. Accurate hybrid stochastic simulation of a system of coupled chemical or biochemical reactions. *The Journal of Chemical Physics*, 122:054103, 2005.